INVESTIGATION OF THE WOUND HEALING ACTIVITY OF TOPICAL GEL EXTRACT OF *CURCUMA AROMATICA* SALISB. (WILD TURMERIC) IN STZ- INDUCED DIABETIC MICE MODEL

UMAR NURA MUHAMMAD

UNIVERSITI SAINS MALAYSIA

2024

INVESTIGATION OF THE WOUND HEALING ACTIVITY OF TOPICAL GEL EXTRACT OF *CURCUMA AROMATICA* SALISB. (WILD TURMERIC) IN STZ- INDUCED DIABETIC MICE MODEL

by

UMAR NURA MUHAMMAD

Thesis submitted in fulfilment of the requirements
for the degree of
Doctor of Philosophy

November 2024

ACKNOWLEDGEMENT

All praise is to Almighty Allah, who taught man what he knows, for sustaining and protecting my life up to this moment. I want to express my sincere gratitude to my supervisor, Dr. Toh Seok-Ming, for her selfless dedication, motherly love, criticisms, corrections, innumerable and unquantifiable support, understanding and perseverance with my shortcomings in guiding me through the tasking process of learning the art of research and all the dynamics involve towards this work's success and its successful completion. I am also indebted with special gratitude to my co-supervisor, Dr. Thaigarajan a/l Parumasivam, for his unflinching interest in the progress of my research and the constant encouragement and invaluable advice he has offered. His readiness to offer any help, moral or financial, is overwhelming, and I am forever grateful.

My special thanks to the head of the Pharmaceutical Technology discipline, Associate Prof. Dr. Chan Siok Yee, the Dean of the School of Pharmaceutical Sciences, USM, Prof. Dr. Habibah A. Wahab, Prof. Dr. Vikneswaran a/l Murugaiyah, and Prof. Gurjeet Kaur Chatar Singh, for their direct and indirect facility, financial and moral supports offered to me, words cannot thank you enough.

Not forgotten and not the least are the most influential people in my life: my parents (Umar Nagwari Tambuwal and Husaina Alkali), wife (Amina Munir), children (Jafar, Arfaan and Jannah), and PhD colleagues (Ahmed, Dayyob, Abdul-Salam, Bilal, and Boon Keate); for the encouragement, sacrifice, moral lessons and education they have strived to impact on my life, thank you for your guidance. Finally, I cannot conclude without sincerely thanking Universiti Sains Malaysia for providing a grant (RUI, 2019, grant number: 1001/PFARMASI/8012341) to support my research work, and I genuinely appreciate all the support.

TABLE OF CONTENTS

ACKNOWLEDGEMENT ..... **ii**
TABLE OF CONTENTS ..... **iii**
LIST OF TABLES ..... **xii**
LIST OF FIGURES ..... **xv**
LIST OF ABBREVIATIONS AND SYMBOLS ..... **xxiv**
LIST OF APPENDICES ..... **xxvii**
ABSTRAK ..... **xxviii**
ABSTRACT ..... **xxxii**
CHAPTER 1 GENERAL INTRODUCTION **1**
1.1 Background 1
1.2 Research Problem 5
1.3 Research Hypothesis 6
1.4 Plants as wound healing agents 7
1.5 Research Question 8
1.6 Aims and Objectives of the Study 8
1.6.1 Aims of the Study 8
1.6.2 Objectives of the Study 8
CHAPTER 2 LITERATURE REVIEW **10**
2.1 Anatomy and function of the human skin 10
2.1.1 Structure of the Skin 11
2.1.1(a) The epidermis layer 11
2.1.1(a)(i) Stratum germinativum 14
2.1.1(a)(ii) Stratum Spinosum (squamous cell layer) 15
2.1.1(a)(iii) Stratum Granulosum (granular cell layer 16
2.1.1(a)(iv) Cornified layer 17
2.1.1(b) Nonkeratinocyte cells of the epidermis 18
2.1.1(b)(i) Merkel cells 18
2.1.1(b)(ii) Langerhans cells 18
2.1.1(b)(iii) Melanocytes 19
2.1.2 The Dermal-Epidermal Junction 20
2.1.3 The Dermis 20
2.1.3(a) The Dermis Vasculature 23
2.1.3(b) Muscles 23
2.1.3(c) Nerves 24

2.1.3(d) Mast Cells 25
2.1.4 The Hypodermis 26
2.1.5 The Epidermal Appendages 27
2.1.5(a) Eccrine sweat glands 27
2.1.5(b) Apocrine Sweat Glands 28
2.1.5(c) Sebaceous glands 29
2.1.5(d) The nails 30
2.1.5(e) Hair Follicles 30
2.2 Physiology of Wound Healing 35
2.2.1 Haemostasis Phase 36
2.2.2 Inflammatory phase 37
2.2.3 Proliferative phase 40
2.2.3(a) Granulation Tissue 40
2.2.3(b) Contraction 43
2.2.3(c) Angiogenesis 44
2.2.3(d) Re-epithelialisation 48
2.2.4 The remodelling phase 50
2.3 Factors Affecting Wound Healing 52
2.3.1 Local Factors Affecting Wound Healing 53
2.3.1(a) Depleted-oxygen supply 53
2.3.1(b) Microbial Infection 54
2.3.2 Systemic factors affecting wound healing 55
2.3.2(a) Ageing 55
2.3.2(b) Diabetes mellitus 56
2.3.2(c) Obesity 58
2.3.2(d) Smoking 59
2.3.2(e) Alcohol Consumption 61
2.3.2(f) Medications 63
2.3.2(f)(i) Non-steroidal Anti-inflammatory Drugs 63
2.3.2(f)(ii) Chemotherapeutics 64
2.3.2(f)(iii) Glucocorticoid Steroids 65
2.3.2(g) Malnutrition 66
2.3.2(g)(i) Carbohydrates and Protein 66
2.3.2(g)(ii) Amino Acids 67
2.3.2(g)(iii) Fatty Acids 68

2.3.2(g)(iv) Vitamins and Micronutrients 69
2.3.3 Wound healing current treatment options and challenges 70
2.3.3(a) Physiologic Wound Healing 71
2.3.3(b) Antimicrobials 72
2.3.3(c) Wound Care and Dressings 74
2.3.3(d) Skin Substitutes 75
2.3.3(e) Negative pressure wound therapy 76
2.3.3(f) Application of growth factors 77
2.3.3(g) Hyperbaric Oxygen Therapy 78
2.3.4 Future Directions 79
2.4 Experimental models of cutaneous wound healing 81
2.5 *Curcuma aromatica* Salisb. 82
2.5.1 Taxonomic classification of *Curcuma aromatica* Salisb. 82
2.5.2 Botanical and Geographical Description of *Curcuma aromatica* Salisb 83
2.5.3 Traditional Uses of *C. aromatica* 84
2.5.4 Phytoconstituents of *C. aromatica* 86
2.5.5 Pharmacological properties of *C. aromatica* 87
CHAPTER 3 PHYTOCHEMICAL SCREENING AND *IN VITRO* ANTIOXIDANT, ANTIBACTERIAL, AND WOUND HEALING ACTIVITIES OF *CURCUMA AROMATICA* SALISB. (*C. AROMATICA*) CRUDE EXTRACTS 97
3.1 Introduction 97
3.2 Materials and Methods 99
3.2.1 Materials and Equipment 99
3.2.1(a) List of Reagents and Chemicals 99
3.2.1(b) Equipment and Apparatus 100
3.3 Methods 101
3.3.1 Preliminary phytochemical analysis of the crude extracts of rhizomes of *Curcuma aromatica* 101
3.3.1(a) Plant material and preparation 101
3.3.1(b) Plant extraction 102
3.3.1(c) Preparation of crude extracts stock solution 102
3.3.1(d) Test for Alkaloids 103
3.3.1(e) Test for flavonoids 103
3.3.1(f) Test for tannings 104

3.3.1(g) Test for Terpenoids and steroids 105
3.3.1(h) Test for phytosterols 105
3.3.2 Quantitative analysis of the crude extracts of rhizomes of *Curcuma aromatica* 106
3.3.2(a) Preparation of crude extracts stock solution 106
3.3.2(b) Preparation of gallic acid standard stock solution 106
3.3.2(c) Preparation of quercetin standard stock solution 106
3.3.2(d) Total phenolic content (TPC) 107
3.3.2(b) Total flavonoid content (TFC) 107
3.4 *In vitro* antioxidant, antibacterial, and wound healing activities of *Curcuma aromatica* Salisb. (*C. aromatica*) 108
3.4.1 *In vitro* antioxidant activity 108
3.4.1(a) Preparation of stock and working solutions 109
3.4.1(a)(i) Preparation of DPPH working solution . 109
3.4.1(a)(ii) Preparation of ABTS working solution . 109
3.4.1(a)(iii) Preparation of FRAP reagent solution ... 109
3.4.1(a)(iv) Preparation of ascorbic acid standard stock solution 110
3.4.1(b) DPPH Radical Scavenging Assay 110
3.4.1(c) ABTS Radical Scavenging Assay 111
3.4.1(d) FRAP Assay 112
3.4.2 *In vitro* antibacterial activity 112
3.4.2(a) Source of bacterial strains 112
3.4.2(b) Broth and Agar preparation 113
3.4.2(c) Agar plate preparation 113
3.4.2(d) Bacterial culture and plate steaking 113
3.4.2(e) Preparation of 0.5 McFarland bacterial suspension ... 114
3.4.2(g) Antibacterial susceptibility test 114
3.4.2(h) Determination of MIC and MBC 115
3.4.2(h)(i) Preparation of stock and working solution of crude extracts of *C. aromatica* rhizome 115
3.4.2(h)(ii) Determination of MIC 116
3.4.2(h)(iii) Determination of MBC 117
3.4.3 *In vitro* wound healing activity 117
3.4.3(a) Cell culture 117

3.4.3(b) Cell passage 118
3.4.3(c) Determination of cell density 119
3.4.3(d) Preparation of crude extracts stock solutions 119
3.4.3(e) MTT Assay 120
3.4.3(f) Scratch wound healing assay 121
3.5 Results and Discussion 123
3.5.1 Preliminary qualitative phytochemical analysis 123
3.5.2 Quantitative analysis of the crude extracts 124
3.5.2(a) Extraction yield 124
3.5.2(b) Total phenolic content (TPC) 127
3.5.2(c) Total flavonoids content (TFC) 129
3.5.3 *In vitro* antioxidant activity 133
3.5.3(a) DPPH Radical Scavenging Assay 133
3.5.3(b) ABTS Radical Scavenging Assay 136
3.5.3(c) FRAP Radical Scavenging Assay 138
3.5.4 *In vitro* antibacterial activity 140
3.5.5 *In vitro* wound healing activity 147
3.5.5(a) MTT Assay 147
3.6.5(b) Scratch wound healing assay 151
CHAPTER 4 METHOD DEVELOPMENT AND VALIDATION OF AN ISOCRATIC REVERSE-PHASE HIGH-PERFORMANCE LIQUID CHROMATOGRAPHY ULTRAVIOLET (HPLC-UV) FOR THE DETERMINATION OF CURCUMINOIDS SIMULTANEOUSLY IN THE CRUDE EXTRACTS OF THE RHIZOMES OF *CURCUMA AROMATICA* SALISB. (*C. AROMATICA*) AND ITS EXTRACT GEL FORMULATION 158
4.1 Introduction 158
4.2 Materials 160
4.2.1 List of Reagents and Chemicals 160
4.2.2 Equipment and Apparatus 160
4.3 Methods 162
4.3.1 Preparation of carbopol gel base 162
4.3.2 Plant extraction 162
4.3.3 Preparation of stock and working solutions 163
4.3.3(a) Preparation of *C. aromatica* ethanolic crude extract stock and working solutions 163

4.3.3(b) Preparation of curcuminoids standard stock and working solutions 163
4.3.4 Method Development 164
4.3.4(a) Optimisation of chromatographic conditions 164
4.3.4(b) Chromatographic instrumentation and conditions .. 164
4.3.4(c) Method validation 165
4.3.4(d) System suitability 165
4.3.4(e) Linearity and Range 166
4.3.4(f) Specificity 166
4.3.4(g) Accuracy 167
4.3.4(h) Precision 168
4.3.4(i) Limits of detection (LOD) and limit of quantitation (LOQ) 168
4.3.4(j) Stock Solution Stability 169
4.3.4(k) Robustness 170
4.3.5 Degradation studies 170
4.3.5(a) Preparation of standard stock solution of curcuminoids standard and curcuminoid gel for degradation studies 171
4.3.5(b) Heat Degradation Study 171
4.3.5(c) Acid and alkali degradation 172
4.3.5(d) Ultraviolet light (UV) degradation 173
4.3.5(e) Hydrogen peroxide oxidative degradation 174
4.3.6 Application of the method 174
4.3.6(a) Determination of curcuminoids in the crude extracts of *C. aromatica* rhizomes 174
4.3.6(b) Recovery of curcuminoid in extract gel formulation of *C. aromatica* rhizomes 175
4.4 Results and Discussion 175
4.4.1 Optimisation of chromatographic conditions 175
4.4.2 System suitability 178
4.4.3 Calibration curve, Linearity and Range 179
4.4.4 Accuracy 181
4.4.5 Precision 181
4.4.6 Specificity 182
4.4.7 Limit of detection (LOD) and Limit of quantitation (LOQ) ... 182
4.4.8 Stock Solution Stability 183

4.4.9 Robustness 183
4.4.10 Degradation studies 184
4.4.11 Application of the developed method 189
4.4.12 Conclusion 189
CHAPTER 5 FORMULATION DEVELOPMENT AND EVALUATION OF NOVEL TOPICAL EXTRACT GEL OF *CURCUMA AROMATICA* SALISB. (*C. AROMATICA*) RHIZOMES FOR WOUND HEALING TREATMENT 191
5.1 Introduction 191
5.2 Materials and Methods 194
5.2.1 Materials and Equipment 194
5.2.1(a) List of Reagents and Chemicals 194
5.2.1(b) Equipment and Apparatus 195
5.3 Methods 196
5.3.1 Plant Material and Preparation 196
5.3.2 Preparation of the *C. aromatica* rhizomes ethanolic extract 196
5.3.3 Quantitative analysis of the crude extract 197
5.3.3(a) Preparation of ethanolic crude extract stock solution 197
5.3.3(b) Preparation of gallic acid standard stock solution 197
5.3.3(c) Preparation of quercetin standard stock solution 197
5.3.3(d) TPC in the *C. aromatica* rhizome extract 198
5.3.3(e) TFC in the *C. aromatica* rhizome 199
5.3.4 Formulation development of ethanolic extract gel of *C. aromatica* rhizomes 200
5.3.4(a) Screening/selection of the gelling agent 200
5.3.4(b) Pre-formulation studies 200
5.3.5 Formulation studies 201
5.3.6 Evaluation of the extract gel formulations 202
5.3.6(a) Organoleptic properties 202
5.3.6(b) pH measurements 202
5.3.6(c) Viscosity 203
5.3.6(d) Spreadability 203
5.3.6(e) Drug content of extract gel formulations 204
5.3.7 Stability studies of the gel formulations 205
5.3.7(a) Organoleptic evaluation 205
5.3.7(b) pH measurements 206

5.3.7(c) Centrifuge test 206
5.3.7(d) HPLC phytochemical stability assay 206
5.4 Results and Discussion 207
5.4.1 Quantitative analysis of the crude extracts 207
5.4.1(a) Extraction yield 207
5.4.1(b) TPC and TFC in the *C. aromatica* rhizome extract 208
5.4.2 Formulation development of ethanolic extract gel of *C. aromatica* rhizomes 209
5.4.2(a) Screening/selection of the gelling agent and Pre-formulation 209
5.4.3 Formulation studies 211
5.4.4 Evaluation of the extract gel formulations 211
5.4.4(a) Physicochemical evaluation 211
5.4.4(b) Accelerated Stability studies of the gel formulations 218
CHAPTER 6 INVESTIGATION OF THE WOUND HEALING EFFECT OF TOPICAL EXTRACT GEL OF *CURCUMA AROMATICA* SALISB. (*C. AROMATICA*) RHIZOMES IN DIABETIC-INDUCED MICE MODEL 227
6.1 Introduction 227
6.2 Materials and Methods 234
6.2.1 Materials and Equipment 234
6.2.1(a) List of Reagents and Chemicals 234
6.2.1(b) Equipment and Apparatus 235
6.3 Methods 236
6.3.1 Experimental animals 236
6.3.2 Acute skin irritation test for the prepared extract gels 236
6.3.3 *In vivo* wound-healing evaluation 239
6.3.3(a) Induction of Diabetes 239
6.3.3(b) Wound creation 240
6.3.3(b)(i) Anesthesia and wound site preparation 240
6.3.3(b)(ii) Excision wound 240
6.3.3(c) Wound treatment 241
6.3.3(d) Histological Study 245
6.3.4 Statistical analysis 246
6.4 Results and Discussion 247
6.4.1 Acute skin irritation test for the prepared extract gels 247

6.4.2 Induction of Diabetes 251
6.4.3 *In vivo* Wound Healing Evaluation 254
6.4.3(a) Effect of *C. aromatica* extract gels on wound contraction rate and percentage of wound closure in diabetic and non-diabetic animals..... 254
6.4.3(b) Histological Study 264
6.5 Conclusion 265
CHAPTER 7 GENERAL CONCLUSIONS AND RECOMMENDATIONS FOR FUTURE RESEARCH..... 268
7.1 General Conclusions 268
7.2 Recommendations for Future Research 275
REFERENCES……276
APPENDICES
LIST OF PUBLICATIONS

LIST OF TABLES

Page

Table 2.1 Pharmacological effects associated with some of the main bioactive compounds identified in *C. aromatica*. 93

Table 3.1 Phytochemical profiling of the ethanolic and hexane crude extracts of *C. aromatica* rhizomes 124

Table 3.2 Percentage yield of ethanol and hexane crude extract of *C. aromatica* rhizomes 126

Table 3.3 Total phenolic and flavonoid content in ethanolic and hexane crude extract of *C. aromatica* rhizomes. 131

Table 3.4 The IC_{50} concentrations of the DPPH radical scavenging assay for the crude ethanolic and hexane extracts of *C. aromatica* rhizomes and standard ascorbic acid (positive control) obtained from their regression equations 135

Table 3.5 The FRAP activity of the standard ascorbic acid (positive control). 140

Table 3.6 Antibacterial susceptibility tests for the ethanolic and hexane crude extracts of *C. aromatica* rhizomes against the tested Gram-negative and Gram-positive bacteria. 146

Table 3.7 The minimum inhibitory concentration (MIC) and minimum bactericidal concentration (MBC) of the crude ethanolic and hexane extracts of *C. aromatica* rhizomes. 146

Table 3.8 The effect of crude ethanolic and hexane extracts of *C. aromatica* rhizomes on the migration of Hs27 fibroblast cells. The initial scratch wound area at time 0 was set at 0%. 152

Table 4.1 Mobile Phase Composition Optimisation and Observation 177

Table 4.2 Results of system suitability studies of curcuminoids. Mean ± SD, *n* = 8. 178

Table 4.3 Accuracy results from the recovery studies of curcuminoid in hydrogel formulation, *n* = 6. 181

Table 4.4 Results of intra-day and inter-day precision. 182

Table 4.5 Results of stress degradation studies of curcuminoid standard..... 187

Table 4.6 Results of stress degradation studies of 5% curcuminoid gel formulation 188

Table 4.7 Comparison of curcuminoid content in the crude extract, extract gel formulation and the curcuminoid standard..... 190

Table 5.1 Composition of the gel formulations of ethanolic extract of *C. aromatica* rhizomes. 202

Table 5.3 Physicochemical Evaluation of Gel Formulations Containing Ethanolic Extract of *C. aromatica* rhizomes. 214

Table 5.4 pH measurements of accelerated stability studies of Gel Formulations Containing Ethanolic Extract of *C. aromatica* rhizomes. 219

Table 5.5a Curcuminoid recovery of accelerated stability studies of the extract gel formulation (F3-1%) containing ethanolic extract of *C. aromatica* rhizomes. 222

Table 5.5b Curcuminoid recovery of accelerated stability studies of the extract gel formulation (F3-10%) containing ethanolic extract of *C. aromatica* rhizomes. 223

Table 6.1 Experimental Animal Groupings and Treatment for Skin Irritation Study 238

Table 6.2 Draize scoring criteria for grading eschar, erythema and oedema as skin irritation. 238

Table 6.3 Experimental Animal Groupings and Treatment for Excision wound-diabetic model group. 244

Table 6.4 Experimental Animal Groupings and Treatment for Excision wound-non-diabetic model group. 244

Table 6.5 Average skin irritation scores for mice in group A treated with dummy gel formulation (F3-blank). 249

Table 6.6 Average skin irritation scores for mice in group B treated with extract gel formulation (F3-1%) containing 1% *C. aromatica* rhizome extract. 249

Table 6.7 Average skin irritation scores for mice in group C treated with extract gel formulation (F3-10%) containing 10% *C. aromatica* rhizome extract. 249

Table 6.8 Evaluation of histological parameters for the assessment of wound healing in the diabetic mice groups. 266

Table 6.9 Evaluation of histological parameters for the assessment of wound healing in the non-diabetic mice groups. 266

LIST OF FIGURES

Page

Figure 2.1 A cross-section of the skin structure showing the three layers of the skin (epidermis, dermis, and hypodermis) and its derivatives (hair, sebaceous, and sweat glands).. 11

Figure 2.2 The four main layers of the epidermis's keratinocyte and other non-keratinocyte cells.. 12

Figure 2.3 Phases of the human hair growth cycle. **A** = Anagen phase, the hair follicle active growth phase, determines the hair length. **B** = Catagen phase is the transition or involution period during which club hair is formed. Also, cell division is terminated at the upper section of the hair follicle, and the hair follicle's lower section starts to involute. **C** = Telogen phase is the resting phase, during which the growing anagen hair shaft gradually pushes out hairs and sheds before new hair develops. **D** = is the early anagen phase after hair sheds; the hair matrix rapidly proliferates and starts new hair formation. 34

Figure 2.4 The pictorial four phases of the wound healing process and the cellular activities involved. 38

Figure 2.5 Cultivated *Curcuma aromatica* Salisb.: whole plant (A), aerial leaves (B), rhizomes and roots (C). 83

Figure 2.6 Chemical structures of some of the main bioactive compounds identified from *C. aromatica.* 96

Figure 3.1 Gallic acid standard curve used for TPC determination in ethanolic and hexane crude extract of *C. aromatica.* 131

Figure 3.2 Quercetin standard curve used for TFC determination in ethanolic and hexane crude extracts of *C. aromatica*. 132

Figure 3.3 The flavonoid basic structure..... 132

Figure 3.4 The DPPH free radical inhibition effect of the crude ethanolic and hexane extracts of *C. aromatica* rhizomes. Each data value represents the mean ± standard deviation (*n* = 3). 135

Figure 3.5 The ABTS free radical inhibition effect of the crude ethanolic and hexane extracts of *C. aromatica* rhizomes. Each data value represents the mean ± standard deviation (*n* = 3). 137

Figure 3.6 FRAP assay showing the reducing ability of the crude ethanolic and hexane extracts of *C. aromatica* rhizomes via increased absorbance. Each data value represents the mean ± standard deviation (*n* = 3). 139

Figure 3.7 The antibacterial susceptibility effect of the various indicated concentrations of the ethanolic crude extract of *C. aromatica* rhizomes in three replications and one positive control against (a) *E. coli*, *Escherichia coli*; (b) P. A, *Pseudomonas aeruginosa*; (c) MRSA, Methicillin-Resistant *Staphylococcus aureus*; and (d) MSSA, Methicillin-Susceptible *Staphylococcus aureus;* over 24 hours of incubation. (e) DMSO, dimethyl sulphoxide; was used as the negative control against all the bacteria (e-1 = *E. coli*, e-2 = *P. aeruginosa*, e-3 = MRSA, e-4 = MSSA). 142

Figure 3.8 The antibacterial susceptibility effect of the various indicated concentrations (H40 = 40 mg/mL, H20 = 20 mg/mL, H10 = 10 mg/mL, and H2 = 2 mg/mL) of the hexane crude extract of *C. aromatica* rhizomes against (a) *E. coli*, *Escherichia coli;* (b) P. A, *Pseudomonas aeruginosa;* (c) MRSA, Methicillin-Resistant *Staphylococcus aureus;* and (d) MSSA, Methicillin-Susceptible *Staphylococcus aureus* over 24 hours of incubation. DMSO, dimethyl sulphoxide, was the negative control against all the tested bacteria (e-1 = *E. coli*, e-2 = *P. aeruginosa*, e-3 = MRSA, e-4 = MSSA). 143

Figure 3.9 Conversion of MTT tetrazolium salt to the purple formazan via hydrogen atom donation by NADH molecule. 149

Figure 3.10(a) Effect of ethanolic crude extract of *C. aromatica* rhizomes on the viability of the Hs27 cell line following incubation with indicated concentrations of the crude extract for 24 hours was determined using the MTT assay. The result data shown in the graph are mean ± standard deviation obtained from triplicate experiments. The cell viability is expressed as a percentage of control (untreated cells). *P < 0.05, **P < 0.01, and ***P < 0.001 compared to control group. 149

Figure 3.10(b) Effect of crude hexane extract of *C. aromatica* rhizomes on the viability of the Hs27 cell line following incubation with indicated concentrations of the crude extract for 24 hours was determined using the MTT assay. The result data shown in the graph are mean ± standard deviation obtained from triplicate experiments. The cell viability is expressed as a percentage of control (untreated cells). *P < 0.05, **P < 0.01, and ***P < 0.001 compared to control group. 150

Figure 3.11 The relative size of the scratch wound or cell-free area. The percentage closure of the scratch wound area was measured after treatment with various indicated concentrations of ethanolic crude extract of *C. aromatica* rhizomes at different time points (0, 6, 12, and 24 hours). *P < 0.05, **P < 0.01, and ***P < 0.001 compared to control group. 153

Figure 3.12 The relative size of the scratch wound or cell-free area. The percentage closure of the scratch wound area was measured after treatment with various indicated concentrations of hexane crude extract of *C. aromatica* rhizomes at different time points (0, 6, 12, and 24 hours). *P < 0.05, **P < 0.01, and ***P < 0.001 compared to control group. 153

Figure 3.13 *In vitro* scratch wound healing assay (X 10 magnification) on Hs27 cell line. (a) The Hs27 fibroblast cells were scratched (cell-free area), left untreated (control) (a), and then treated with 12.5 µg/mL of crude ethanolic extract (b) and 12.5 µg/mL of crude

hexane extract (c) of *C. aromatica* rhizomes. The crude ethanolic extract showed excellent cell proliferation and migration within the treatment period (24 hours) at the indicated concentration compared to crude hexane extract and control (untreated)..... 155

Figure 3.14 *In vitro* scratch wound healing assay (X 10 magnification) on Hs27 cell line. (a) The Hs27 fibroblast cells were scratched (cell-free area), left untreated (control) (a), and then treated with 25 µg/mL of crude ethanolic extract (b) and 25 µg/mL of crude hexane extract (c) of *C. aromatica* rhizomes. The crude ethanolic extract showed good cell proliferation and migration within the treatment period (24 hours) at the indicated concentration compared to crude hexane extract and control (untreated). 156

Figure 3.15 *In vitro* scratch wound healing assay (X 10 magnification) on Hs27 cell line. (a) The Hs27 fibroblast cells were scratched (cell-free area), left untreated (control) (a), and then treated with 50 µg/mL of crude ethanolic extract (b) and 50 µg/mL of crude hexane extract (c) of *C. aromatica* rhizomes. The crude ethanolic extract showed moderate cell proliferation and migration within the treatment period (24 hours) at the indicated concentration compared to crude hexane extract and control (untreated)..... 157

Figure 4.1 Chemical structures of the three curcuminoids found in the rhizomes of *C. aromatica* 159

Figure 4.2 Chromatogram of a curcuminoid reference sample under the optimised conditions of the proposed method, showing peaks for CUR (a), DMC (b), and BDMC (c), with their respective retention times..... 177

Figure 4.3 Calibration curve plot of CUR at eight concentration levels..... 179

Figure 4.4 Calibration curve plot of DMC at eight concentration levels..... 180

Figure 4.5 Calibration curve plot of BDMC at eight concentration levels ... 180

Figure 4.6a Chromatogram of blank solvent used for the stress degradation test showing the solvent peak and retention time..... 185

Figure 4.6b Chromatogram of placebo sample for acid hydrolysis stress test. 185

Figure 4.6c Chromatogram of a curcuminoid standard solution at 125 µg/mL under acid (3M HCl) degradation stress, showing peaks for CUR (a), DMC (b), and BDMC (c), with their respective retention times, separated from degradation product peaks. 186

Figure 4.6d Chromatogram of an unstressed curcuminoid standard solution at 125 µg/mL showing peaks for CUR (a), DMC (b), and BDMC (c), with their respective retention times. 186

Figure 4.7 Comparative chromatograms of the analysed *C. aromatica* rhizome extract (10 mg/mL), extract gel formulation (10 mg/mL) and the curcuminoid standard (7.81 µg/mL) showing peaks for curcumin (a), demethoxycurcumin (b) and bis-demethoxycurcumin (c) and their respective retention time. 190

Figure 5.1 F3 (1% Carbopol 940) gel base on a benchtop at room temperature 211

Figure 5.2 Physical appearance of the formulated extract gels containing different concentrations of *C. aromatica* rhizome extract. 213

Figure 5.3 Spreadability profiles of the formulated extract gels containing different concentrations of *C. aromatica* rhizome extract. 214

Figure 5.4a Effect of shear rate on the viscosity of the extract gel formulation F3-1%. 216

Figure 5.4b Effect of shear rate on the viscosity of the extract gel formulation F3-10%. 216

Figure 5.5a HPLC chromatographic profile of curcuminoids, curcumin (a), demethoxycurcumin (b) and bis-demethoxycurcumin and their retention times, detected in the pure crude extract of *C. aromatica* rhizome extract. 224

Figure 5.5b HPLC chromatographic profile of curcuminoids, curcumin (a), demethoxycurcumin (b) and bis-demethoxycurcumin and their retention times, detected solution of extract gel formulation (F3-1%) at different time points under storage condition of 4 °C of accelerated studies. 224

Figure 5.5c HPLC chromatographic profile of curcuminoids, curcumin (a), demethoxycurcumin (b) and bis-demethoxycurcumin and their retention times, detected solution of extract gel formulation (F3-1%) at different time points under storage condition of 24 - 31 °C/75% RH of accelerated studies. 225

Figure 5.5d HPLC chromatographic profile of curcuminoids, curcumin (a), demethoxycurcumin (b) and bis-demethoxycurcumin and their retention times, detected solution of extract gel formulation (F3-10%) at different time points under storage condition of 4 °C of accelerated studies. 225

Figure 5.5e HPLC chromatographic profile of curcuminoids, curcumin (a), demethoxycurcumin (b) and bis-demethoxycurcumin and their retention times, detected solution of extract gel formulation (F3-10%) at different time points under storage condition of 24 - 31 °C/75% RH of accelerated studies. 226

Figure 6.1 Representation of bilateral excision wounds in mice model. The left wound (L) was used as the control and treated with the formulation vehicle control (F3-blank). The right wound (R) was used as the drug testing site and treated with either of the formulated extract gels (F3-1% and F3-10%). 243

Figure 6.2 Observation of skin irritation signs post-application of the tested gels (F3-blank, F3-1%, and F3-10%) on the shaved skin area of the mice in various groups and at different time intervals. 250

Figure 6.3 Histological view of acute skin irritation test showing no significant changes in mice skin texture on the application of the formulated extract gels F3-1% (C) and F3-10% (D) prepared from

C. aromatica rhizomes and dummy gel, F3-blank (B) when compared to an intact, untreated mice skin (A). [40× manification, scale bar 100 µm]. 251

Figure 6.4 Average blood glucose levels in streptozotocin (STZ) diabetes-induced mice (diabetic group) and the control group (non-diabetic mice). 253

Figure 6.5 Initial and final average body weights of the streptozotocin (STZ) diabetes-induced mice (diabetic group) and non-diabetic mice (control group). 253

Figure 6.6 Macroscopic observation of the wound healing process from the wounding day (Day 0) to the last day of treatment (Day 14) in the diabetic mice groups. "**A**" represents the left wound treated with a dummy gel (F3-blank), whereas "**B**" represents the right wound treated with the formulated *C. aromatica* extract gels, either extract gel F3-1% or F3-10%. Both wounds (left and right) in the negative control group were left untreated, but in the positive control group, the two wounds (left and right) were both treated with 10% povidone-iodine. DNC, diabetic negative control; DTG1, diabetic test group 1; DTG2, diabetic test group 2; DPC, diabetic positive control. 256

Figure 6.7a Effect of topical treatment with an extract gel formulation containing 1% *C. aromatica* rhizomes extract on the skin wound area in streptozocin-induced diabetic mice. The results are expressed as mean ± standard error of the mean (n = 6/group). The ** indicates $p < 0.01$, *** indicates $p < 0.001$ vs placebo control by ordinary one-way ANOVA (post-Tukey's multiple comparisons test). DTG-1 = diabetic test group 1, DG = dummy gel, DNC = diabetic negative control, F3-1% = extract gel 1%, and DPC = diabetic positive control. 257

Figure 6.7b Effect of topical treatment with an extract gel formulation containing 10% *C. aromatica* rhizomes extract on the skin wound area in streptozocin-induced diabetic mice compared to F3-blank

(formulation control), untreated (negative control), and 10% povidone-iodine (positive control). The results are expressed as mean ± standard error of the mean (n = 5/group). The *** indicates $p < 0.001$ vs. placebo control by ordinary one-way ANOVA (post-Tukey's multiple comparisons test). DTG-2 = diabetic test group 2, DG = dummy gel, DNC = diabetic negative control, F3-10% = extract gel 10%, and DPC = diabetic positive control..... 257

Figure 6.8 Macroscopic observation of the wound healing process from the wounding day (Day 0) to the last day of treatment (Day 10) in the non-diabetic mice group. "**A**" represents the left wound treated with a dummy gel (F3-blank), whereas "**B**" represents the right wound treated with the formulated extract gels, either extract gel F3-1% or F3-10%. Both wounds (left and right) in the negative control group were left untreated, but in the positive control group, the two wounds (left and right) were both treated with 10% povidone-iodine. NDNC, non-diabetic negative control; NDTG1, non-diabetic test group 1; NDTG2, non-diabetic test group 2; NDPC, non-diabetic positive control..... 260

Figure 6.9a Effect of topical treatment with an extract gel formulation (F3-1%) containing 1% *C. aromatica* rhizomes extract on the skin wound area in non-diabetic mice compared to F3-blank (formulation control), untreated (negative control) and 10% povidone-iodine (positive control). The results are expressed as mean ± standard error of the mean (n = 6/group). The ** indicates $p < 0.005$ vs placebo (F3-blank treated) and untreated controls, respectively, by ordinary one-way ANOVA (post-Tukey's multiple comparisons test). 262

Figure 6.9b Effect of topical treatment with an extract gel formulation (F3-10%) containing 10% *C. aromatica* rhizomes extract on the skin wound area in non-diabetic mice compared to F3-blank (formulation control), untreated (negative control) and 10% povidone-iodine (positive control). The results are expressed as

mean ± standard error of the mean (n = 6/group). The ** indicates p <0.005, and *** indicates p <0.001 vs placebo (F3-blank treated) and untreated controls, respectively, by ordinary one-way ANOVA (post-Tukey's multiple comparisons test). 262

Figure 6.10 Histological evaluation of diabetic and non-diabetic mice healed skin sections stained with hematoxylin and eosin (scale bar = 100 μm). NGC, negative control group (untreated); F3-blank (formulation vehicle control); F3-1% (formulated extract gel containing 1% of *C. aromatica* rhizome extract); F3-10% (formulated extract gel containing 10% of *C. aromatica* rhizome extract); 10% PI, 10% povidone-Iodine (positive control); nEP, neo-epidermal; EP, epidermis; IC, infiltration cells; G, granulation tissue; U, ulcer; DR, dermis; HF, hair follicles; FB, fibroblast; I, inflammation. 267

LIST OF ABBREVIATIONS AND SYMBOLS

°C	Degree celsius
ABTS	2,2-azino-bis-3-ethylbenzothiazoline-6-sulphonic acid
ANOVA	Analysis of variance
AP	Arrector pili
ATCC	American type culture collection
COX2	Cyclooxygenase-2
DMSO	Dimethylsuphuroxide
DMEM	Dulbeccos Modified Eagle Medium
DPPH	2,2-Diphenyl-1-picrylhydrazyl
e.g.	exempli gratia
ECM	Extracellular matrix
FDA	United States Food and Drug Administration
FRAP	Ferric reducing antioxidants power
Fe-TPTZ	Ferrous-tripyridyltriazine
h	Hour
HPLC	High Performance Liquid Chromatography
Hs27	Human foreskin fibroblast cell line
i.e.	That is; in other words
ICH	International Conference on Harmonization

IL	Interleukin
LOD	Limit of Detection
LOQ	Limit of Quantification
MMPs	Matrix metalloproteinases
M	Molar
MHA	Mueller-Hilton agar
mg	Milligram
MCP-1	Monocyte Chemoattractant Protein-1
MIC	Minimum inhibitory concentration
MBC	Minimum bactericidal concentration
min	Minute
mL	Milliliter
mm	Millimeter
N	Theoretical plates
nm	Nanometer
NSAIDs	Non-steroidal anti-inflammatory drugs
PEG	Poly(ethylene glycol)
RE	Relative Error
RH	Relative Humidity
rpm	Rotation per minute

ROS	Reactive oxygen species
RSD	Relative Standard Deviation
SD	Standard deviation
STZ	Streptozotocin
TEA	Triethanolamine
TNF-α	Tumor Necrosis Factor-alpha
TGF-β	Transforming Growth Factor-Beta
TPC	Total phenolic content
TFC	Total flavonoid content
UK	United Kingdom
USP	United States Pharmacopoeia
UV	Ultraviolet
UV-VIS	Ultraviolet-Visible
v/v	Volume by Volume
VEGF	Vascular endothelial growth factor
w/v	Weight by Volume
µg/mL	Microgram per milliliter
µL	Microliter
%	Percent

LIST OF APPENDICES

Appendix A	Results of the robustness evaluation for the deleloped HPLC method
Appendix B	Animal Ethics Approval
Appendix C	One-way ANOVA followed by Tukey's Multiple Comparison Test for the *in vivo* diabetic wound healing analysis of the present study
Appendix D	One-way ANOVA followed by Tukey's Multiple Comparison Test for the *in vivo* non-diabetic wound healing analysis of the present study
Appendix E	Herbarium specimen voucher for identification and authentication of *C. aromatica*
Appendix F	Turnitin Originality Report
Appendix G	Certificate of pre-viva presentation

KAJIAN AKTIVITI PENYEMBUHAN LUKA GEL TOPIKAL EKSTRAK *CURCUMA AROMATICA* SALISB. (KUNYIT LIAR) DALAM MODEL TIKUS DIABETES DIARUH STZ

ABSTRAK

Penyembuhan luka adalah proses biologi yang kompleks yang memerlukan serangkaian fasa fisiologi serentak, seperti hemostasis, keradangan, proliferasi (granulasi dan epitelisasi) dan pengubahsuaian (maturation). Proses penyembuhan ini diselaraskan oleh mekanisme selular dan molekul yang rumit melibatkan pelbagai faktor pertumbuhan dan sitokin. Namun, penyakit metabolik kronik seperti diabetes mellitus diketahui menyebabkan luka kronik yang tidak sembuh seperti ulser kaki diabetes dan ulser tekanan. Patofisiologi luka kronik sering melibatkan ketidakseimbangan redoks dan disfungsi laluan keradangan, kadangkala dengan jangkitan mikroba serentak. Ketidakseimbangan redoks adalah fenomena yang meningkatkan pengeluaran radikal bebas dan mengurangkan mekanisme pertahanan antioksidan dalam badan, seperti yang dilihat dalam ulser kaki diabetes dan ulser tekanan di mana antioksidan endogen seperti glutation dan tokoferol berkurangan dengan ketara atau tiada, menunjukkan ketidakseimbangan oksidatif yang teruk yang menyebabkan kecederaan tisu dikenali sebagai tekanan oksidatif melalui peroksidasi lipid membran dan pengoksidaan protein dan enzim penting. Oleh sebab itu, terdapat minat yang semakin meningkat dalam kajian farmaseutikal penyembuhan luka baru yang mengandungi ekstrak tumbuhan dengan sebatian yang mempunyai sifat penyingkiran radikal bebas yang boleh memperbaiki penyembuhan luka dengan berkesan dan ketara serta melindungi daripada tekanan oksidatif. Penyelidikan semasa ini memberi tumpuan kepada pembangunan dan penilaian gel ekstrak rizom

Curcuma aromatica (*C. aromatica*) untuk penyembuhan luka dalam model tikus diabetes dan bukan diabetes. Kajian ini juga menilai aktiviti antioksidan, antibakteria, dan penyembuhan luka ekstrak tersebut. Ekstrak kasar etanol menunjukkan aktiviti penyingkiran radikal DPPH, ABTS dan FRAP yang lebih tinggi berbanding ekstrak kasar heksana, mungkin disebabkan oleh kandungan fenolik dan flavonoid total yang lebih tinggi. Ekstrak kasar etanol menunjukkan aktiviti antibakteria yang bergantung kepada kepekatan terhadap bakteria Gram-negatif dan Gram-positif, termasuk *P. aeruginosa*, MRSA, dan MSSA. Namun, *E. coli* adalah tahan. Penyembuhan luka *in vitro* sel Hs27 yang dirawat dengan pelbagai kepekatan ekstrak mentah *C. aromatica* dan kawalan yang tidak dirawat menunjukkan bahawa kepekatan terendah ekstrak mentah etanol secara signifikan merangsang migrasi sel dan menunjukkan penyembuhan lengkap 24 jam selepas rawatan. Namun, ekstrak mentah heksana menunjukkan aktiviti migrasi dan proliferasi yang lebih perlahan, menunjukkan toksisiti yang tinggi. Kaedah penunjuk kestabilan HPLC-UV fasa terbalik isokratik yang dibangunkan untuk penentuan serentak curcumin, demethoxycurcumin, dan bisdemethoxycurcumin dalam ekstrak etanol mentah rimpang *C. aromatica* telah disahkan mengikut garis panduan ICH dan digunakan buat kali pertama dalam penentuan serentak kurkuminoid dalam ekstrak rimpang *C. aromatica*. Kaedah ini menunjukkan kekhususan yang tinggi dan keupayaan penunjuk kestabilan, berjaya mengenal pasti puncak analit dan produk penguraian. Kaedah HPLC yang dibangunkan adalah mudah, kos efektif, dan sesuai untuk analisis rutin formulasi atau produk kurkuminoid. Ekstrak etanol dari rizom *C. aromatica* menunjukkan aktiviti farmakologi yang kuat in vitro dan oleh itu digunakan dalam formulasi gel ekstrak topikal untuk rawatan penyembuhan luka. Pangkalan gel Carbopol 940 adalah yang paling konsisten dan telus daripada semua

polimer penggelling yang diuji dan oleh itu digunakan dalam penyediaan formulasi gel ekstrak. Formulasi gel ekstrak, F3-1% dan F3-10% yang mengandungi 1% dan 10% ekstrak rimpang *C. aromatica*, telah dipilih untuk penilaian lanjut. Formulasi gel ekstrak mengekalkan hampir 100% kandungan ubat setiap gram gel selama tiga bulan, memastikan potensi penyembuhan luka mereka. Formulasi gel ekstrak diuji pada kulit tikus untuk penilaian kerengsaan kulit akut, menunjukkan tiada bengkak yang ketara, reaksi keradangan, eritema, pembentukan eschar, atau anomali lain. Keberkesanan *in vivo* bagi formulasi gel ekstrak yang diformulasi telah dinilai dengan merawat luka eksisi pada tikus diabetes dan bukan diabetes dengan formulasi tersebut sekali sehari. Kajian mendapati bahawa formulasi gel ekstrak *C. aromatica* mempercepatkan penyembuhan luka dengan ketara pada tikus diabetes dan bukan diabetes berbanding dengan tikus yang tidak dirawat dan tikus kawalan formulasi. Kompaun fenolik dalam ekstrak, khususnya kurkuminoid, telah dikenalpasti sebagai kompaun aktif utama dalam ekstrak etanol *C. aromatica* yang dikaji dan berpotensi bertanggungjawab terhadap aktiviti penyembuhan luka formulasi gel ekstrak tersebut. Kajian histologi terhadap biopsi eksisi luka kulit pada hari ke-14 untuk kumpulan tikus diabetes dan hari ke-10 untuk kumpulan tikus bukan diabetes menunjukkan struktur kulit yang diperbaiki dengan epitelialisasi normal, pemulihan folikel rambut, dan fibrosis dermis yang ketara dalam kumpulan F3-1% dan F3-10%, serta kumpulan yang dirawat dengan povidone-iodine, menunjukkan penyembuhan yang lengkap. Formulasi gel ekstrak yang dibangunkan adalah sesuai untuk rawatan penyembuhan luka yang berkesan pada tikus diabetes dan bukan diabetes. Sejauh pengetahuan kami, kajian ini adalah penyelidikan saintifik sistematik pertama mengenai aktiviti penyembuhan luka ekstrak etanol rizom *C. aromatica* dan

formulasi hidrogelnya yang mengesahkan dakwaan tradisional penyembuhan luka *C. aromatica*.

INVESTIGATION OF THE WOUND HEALING ACTIVITY OF TOPICAL GEL EXTRACT OF *CURCUMA AROMATICA* SALISB. (WILD TURMERIC) IN STZ- INDUCED DIABETIC MICE MODEL

ABSTRACT

Wound healing is a complex biological process that requires a series of concurrent physiological phases, such as haemostasis, inflammation, proliferation (granulation and epithelialisation) and remodelling (maturation). This healing process is coordinated by complicated cellular and molecular mechanisms involving different growth factors and cytokines. However, chronic metabolic diseases such as diabetes mellitus are known to cause chronic, non-healing wounds such as diabetic foot ulcers and pressure ulcers. Chronic wound pathophysiology often involves redox imbalance and inflammatory pathway dysregulation, sometimes with concurrent microbial infection. Redox imbalance is a phenomenon that increases free radical production and decreases the antioxidant defence mechanism in the body, as seen in diabetic foot ulcers and pressure ulcers where endogenous antioxidants like glutathione and tocopherols are significantly reduced or absent, indicating a severe oxidative imbalance causing tissue injury known as oxidative stress via lipid peroxidation of membranes and oxidation of essential proteins and enzymes. For this reason, there is a growing interest in the study of new wound-healing pharmaceuticals containing plant extracts having compounds with free radical scavenging properties that can effectively and significantly improve wound healing and protect against oxidative stress. This current research focuses on developing and evaluating an extract gel of *Curcuma aromatica* (*C. aromatica*) rhizomes for wound healing in diabetic and non-diabetic mice models. The study also evaluated the

extracts' antioxidant, antibacterial, and wound-healing activities. The ethanolic crude extract demonstrated higher DPPH, ABTS and FRAP radical scavenging activity than the hexane crude extract, possibly due to its higher total phenolic and flavonoid content. The ethanolic crude extract showed a concentration-dependent antibacterial activity against Gram-negative and Gram-positive bacteria, including *P. aeruginosa*, MRSA, and MSSA. However, *E. coli* was resistant. *In vitro* wound healing of Hs27 cells treated with different concentrations of *C. aromatica* crude extracts and untreated control showed that the lowest concentration of the ethanolic crude extract significantly stimulated cell migration and exhibited complete healing 24 hours post-treatment. However, the hexane crude extract showed slower migration and proliferation activity, demonstrating high toxicity. The developed isocratic reverse-phase HPLC-UV stability-indicating method for the simultaneous determination of curcumin, demethoxycurcumin, and bisdemethoxycurcumin in the crude ethanolic extract of *C. aromatica* rhizomes was validated as per ICH guidelines and applied for the first time in the simultaneous determination of curcuminoids in the rhizome extract of *C. aromatica*. The method demonstrated high specificity and stability-indicating capability, successfully identifying analyte and degradation product peaks. The developed HPLC method was simple, cost-effective, and suitable for routine analysis of curcuminoid formulations or products. The ethanolic extract of *C. aromatica* rhizome demonstrated potent pharmacological activity *in vitro* and thus was used in topical extract gel formulations for wound healing treatment. Carbopol 940 gel base was the most consistent and transparent of all the gelling polymers tested and was therefore used in extract gel formulation preparation. The extract gel formulations, F3-1% and F3-10% containing 1% and 10% *C. aromatica* rhizome extract, were selected for further evaluation. The extract gel formulations retained

nearly 100% drug content per gram of gel over three months, ensuring their wound-healing potential. The extract gel formulations were tested on mice skin for acute skin irritation evaluation, showing no visible swelling, inflammatory reactions, erythema, eschar formation, or other anomalies. The *in vivo* effectiveness of the formulated extract gel formulations was evaluated by treating an excision wound on diabetic and non-diabetic mice with the formulation once a day. The study found that the *C. aromatica* extract gel formulations significantly accelerated wound healing in diabetic and non-diabetic mice compared to untreated and formulation control mice. The phenolic compounds in the extract, specifically curcuminoids, were identified as the main active compounds in the investigated ethanolic extract of *C. aromatica* rhizomes and could potentially be responsible for the wound-healing activity of the extract gel formulation. The histological study of a skin wound excision biopsy on day 14 for diabetic and day 10 for non-diabetic mice groups showed repaired skin structures with normal epithelialisation, hair follicle restoration, and significant dermis fibrosis in the F3-1% and F3-10%, and povidone-iodine-treated groups, indicating complete healing. The developed extract gel formulation is suitable for effective wound-healing treatment in diabetic and non-diabetic mice. To the best of our knowledge, this study is the first systematic scientific investigation of the wound-healing activity of *C. aromatica* rhizome ethanolic extract and its hydrogel formulation that validated the traditional wound-healing claim of *C. aromatica*.

CHAPTER 1

GENERAL INTRODUCTION

1.1 Background

Wounds are injuries due to physical, chemical or microbial agents that disrupt the normal anatomic structure and cause loss of tissue function (Singh *et al*., 2017). Thus, proper wound healing is necessary to restore tissue integrity and physiological function. Wounds are classified as open or closed wounds (based on aetiology) and acute or chronic wounds (based on the physiology of the healing process). In open wounds, the skin is cut, exposing the underlying tissue to the outside environment, making the wounds vulnerable to infection. Examples of open wounds include incised wounds, lacerations or tear wounds, abrasions or superficial wounds, avulsions, puncture wounds, penetration wounds and gunshot wounds. In contrast, closed wounds are the opposite, but the damage can still affect the underlying tissues, muscles, internal organs, and bones. Closed wounds include bruises, blood tumours, crush injuries, and many more (Percival, 2002; Lazarus *et al*., 1998).

An acute wound is a tissue injury that quickly activates and passes through coordinated physiological wound-healing phases (haemostasis, inflammation, proliferation and tissue remodelling). In contrast, a chronic wound is a tissue injury that demonstrates a delayed or prolonged healing process in most cases due to pathological inflammation (Lukanc et al., 2018; Singh et al., 2017), thereby preventing the wound from progressing into the proliferative phase (Wang *et al*., 2018). Hence, this results in delayed wound healing, consequently causing reduced quality of life, leading to increased morbidity and mortality rates and poor cosmetic outcomes (Sami et al., 2019; Singh et al., 2017). Wounds are termed chronic if they

do not heal within three months (Singh et al., 2017; Tricco et al., 2015) after the onset of the wound.

Most chronic wounds are ulcerative, including vascular, diabetic, and pressure ulcers (Singh et al., 2017; Wong et al., 2015). Studies by Aly (2012) and Guo and DiPietro (2010) discovered that systemic factors such as diabetes mellitus, age, obesity, smoking, alcoholism, medication, and nutrition deficiency might impair wound healing. People with diabetes are more prone to wound infection, and it has been reported that the incidence is 11% higher than in the general population (Nagori and Solanki, 2011). This claim is worrying because of the enormous increase in the diabetic adult population annually, as contained in a 2016 World Health Organization (WHO) report that more than 420 million adults were living with diabetes in 2014, as against the 108 million in 1980, reported by Muniandy *et al*. (2018).

Diabetes mellitus is becoming more common due to an ageing population. It is estimated that approximately 617 million people globally are 65 years old or older. That equates to more than 8.5 per cent of the global population (Ariyanchira, 2017). This figure is predicted to rise to 1.6 billion by 2050. It is also reported that chronic wounds are commonly found among elderly patients aged 65 years and above (Sen, 2023). Diabetic foot ulcers and necrotising fasciitis in the elderly are among the leading causes of hospitalisation in the older population, necessitating intensive wound care and prolonged wound dressing (Ariyanchira, 2017).

Management of chronic wounds is one of the significant public health challenges, and little is known about their actual burden on the healthcare system (Singh et al., 2017); such wounds will continue to have a severe impact on quality of

life, cost of healthcare to patients and healthcare institutions around the globe with the ever-growing population (Agyare *et al*., 2016). It is estimated that about 1 to 2% of the population of high-economy countries will have a chronic wound during their lifetime (Järbrink *et al*., 2016; Nussbaum *et al*., 2018). Interestingly, in the United States of America (USA) alone, it is estimated that over 6.5 million people (i.e. about 2 % of the total population) suffer from chronic wounds (Lordani *et al*., 2018; Mathieu *et al*., 2006; Menke *et al*., 2007; Mohanty and Sahoo, 2017). In contrast to the United Kingdom (UK), Denmark, and Sweden, 1% of their population has a chronic wound, as Walton (2014) reported.

As a result, North America has spent over US$25 billion per year on the management of chronic wounds (Shedoeva *et al*., 2019), while over £5 billion is spent annually by the National Health Service (NHS) in the UK on the care of patients with chronic wounds (Ahmajärvi *et al*., 2019; Guest *et al*., 2015, 2017). Similarly, Australia's annual cost of managing three common chronic wounds (pressure, leg, and diabetic foot ulcers) is US$2.85 billion (Kapp and Santamaria, 2017). In Denmark, chronic wound care poses a financial burden of €99 million per year and is expected to rise by 30 % in the next decade (Hjort and Gottrup, 2010). Furthermore, in developing countries like Malaysia, the Ministry of Health estimated that the annual expenditure for chronic wound care in Malaysia is around US$5 million (Ariyanchira, 2017). The figure is expected to be more prominent in the coming years due to the slow but steady increase in the Malaysian diabetic population, reportedly around 3.5 million (Muniandy *et al*., 2018).

Globally, wound care costs averaged US$2.8 billion annually as of 2014 and are anticipated to reach US$3.5 billion in 2021 (Settipalli, 2015). However, according to a market research report in 2018, the global market for wound closure

products will surpass US$15 billion before the end of the year 2022, and by 2024, the market for advanced wound care aimed at chronic ulcers and surgical wounds is projected to exceed US$22 billion as reported by Sen (2019). Thus, it has become evident that chronic wound treatment has a significant economic impact on the public and warrants more attention.

Traditional medicines produced from indigenous plants, animals, and natural products are the mainstay of wound care for millions throughout Asia, Africa, the Middle East, and Latin America (Shedoeva *et al*., 2019). For this reason, Traditional and Complementary Medicine (TCM) has gained wide acceptance even amongst the elite conventional medical practitioners as a vital component of the current primary healthcare system in many developing and developed countries. For example, Siti *et al*. (2009) reported that 69.4% of Malaysians use TCM daily in Malaysia. Hence, the Ministry of Health Malaysia has implemented proactive policies to promote TCM incorporation in the healthcare scheme to complement conventional medications and urge research institutions to research the safety and efficacy of TCM (Siti *et al*., 2009). For example, in 2001, the Malaysian government expressed its determination to promote and regulate TCM by publishing the National Policy on Traditional/Complementary Medicine. In the Policy, the government declared the institutionalization, professionalization, and integration of TCM into the national health care system (NHS) in the name of quality and safety (Park *et al*., 2022). Similarly, the World Health Organization (WHO) mentioned that ethnomedicinal plant research merits more attention (Benzi and Ceci, 1997) due to the plethora of natural bioactive constituents of plant origin proven to possess therapeutic effects in managing a broad spectrum of diseases.

Undeniably, herbal therapy has been pivotal in wound healing and other skin ailments (Agyare *et al*., 2016). In addition, plants with wound-healing properties have served as alternative forms of treatment in managing wounds, particularly in rural settings (Sabale *et al*., 2012). In this study, one folkloric medicinal plant, *Curcuma aromatica* Salisb (*C. aromatica*), used in traditional medicine, will be explored for pharmacological validation of its efficacy in treating diabetic wounds.

C. aromatica is a Zingiberaceae family member, genus *Curcuma*. *C. aromatica* is an annual herb with a light yellow rhizome found throughout the tropics and subtropics of the world. It is cultivated chiefly for its rhizomes in Asian countries, including China, India, and Japan (Umar *et al*., 2020). In English, *C. aromatica* is known as wild turmeric, whereas in Hindi, it is called *Jangli Haldi* and *Yujin* in Chinese. The rhizomes of *C. aromatica* are used in traditional medicine to treat blood stasis, slow ageing, alleviate pain, and protect against liver disease (Dosoky and Setzer, 2018). The rhizomes are also consumed as a tonic and carminative and are also applied topically for various skin diseases, such as sprains and bruises, as an antidote for snake venom, and to enhance the complexion tone (Ahmad *et al*., 2011; Dosoky and Setzer, 2018; Preethi *et al*., 2010; Xiang *et al*., 2017). In the North-Eastern portion of India, aqueous extracts and paste (made with milk) of *C. aromatica* rhizomes and leaves are, among other things, used to treat indigestion, rheumatism, diarrhoea, used topically for wound healing and prevention of helminth infections (Sikha *et al*., 2015).

1.2 Research Problem

Chronic metabolic diseases such as diabetes mellitus are known to cause chronic, non-healing wounds such as diabetic foot ulcers. It is estimated that the lifetime

probability of people with diabetes developing a chronic foot ulcer is around 10–25% (Dargaville *et al*., 2013; Margolis *et al*., 2011). It is also worth noting that diabetes is the leading cause (90%) of nontraumatic leg amputations in the USA (Dargaville *et al*., 2013). Apart from diabetes, the global prevalence of pressure ulcers in critical and intensive care patients is also increasingly alarming and reported to be around 33%, and about 50–80% of such cases were hospital-acquired (Anthony *et al*., 2019; Dreifke *et al*., 2015; Shahin *et al*., 2008). Diabetic foot and pressure ulcers are the root cause of morbidity, and their care is a massive financial burden (Dreifke *et al*., 2015). Therefore, the progressive increase in diabetes mellitus, an ageing population, and the high demand for wound care have renewed interest in investigating new, affordable, safe, and effective healing therapies from natural sources.

1.3 Research Hypothesis

Chronic wound pathophysiology often involves redox imbalance and inflammatory pathway dysregulation, sometimes with concurrent microbial infection. Endogenous antioxidants like glutathione and tocopherols are significantly reduced or absent, indicating a severe oxidative imbalance causing tissue injury known as oxidative stress via lipid peroxidation of membranes and oxidation of essential proteins and enzymes (Johnson *et al*., 2021; Shetty, 2012). Redox imbalance is a phenomenon that increases free radical production and decreases the antioxidant defence mechanism in the body (Cheeseman, 1993). Oxygen-free radicals are produced principally in inflamed or ischemic tissues during the inflammatory response (S. Singh et al., 2017). This activity is seen in diabetic foot ulcers and pressure ulcers as they are always accompanied by hyperglycemia and hypoxia, which increase oxygen-free radicals concentrations (Guo and DiPietro, 2010).

Our research hypothesis is that topical applications of compounds with free radical scavenging properties can effectively and significantly improve wound healing and protect against oxidative stress.

1.4 Plants as wound healing agents

Plants containing carotenoids and polyphenolic flavonoids have potent antioxidant and wound-healing properties (Agyare *et al*., 2016). Furthermore, as natural free radical scavengers, flavonoids have been reported to inhibit lipid peroxidation and promote vascular relaxation to accelerate wound healing (Govindarajan *et al*., 2004; Shetty, 2012). Lastly, many polyphenols have antibacterial properties, which can help prevent or resolve local wound infections (J. B. Johnson et al., 2021). Some of these plants' acute wound-healing activity has been scientifically screened and evaluated in various pharmacological models. However, most of these medicinal plants' potential in chronic wound healing has yet to be explored (Chopda and Mahajan, 2009), and active chemical constituents were identified only in a couple of cases (Ahmad *et al*., 2011; Govindarajan *et al*., 2004).

Previous studies have reported beneficial pharmacological properties of *C. aromatica*, such as antioxidant, antimicrobial, anti-inflammatory, anticancer, antidiabetic, antitussive, antiobesity, antiangiogenic and immunological effects (Birdane *et al*., 2018; Pant *et al*., 2013; Preethi *et al*., 2010; Revathi and Malathy, 2013). However, to our knowledge, no scientific data has been reported to support its traditional wound-healing activity. Therefore, *C. aromatica* was selected as the plant of interest in this study because of its multi-therapeutic potential.

1.5 Research Question

This research investigates whether extract gels of *C. aromatica* rhizomes can effectively and safely cure cutaneous wounds in a diabetic mice model.

1.6 Aims and Objectives of the Study

1.6.1 Aims of the Study

This research aims to formulate an extract gel of *C. aromatica* rhizomes and assess its wound healing activity on the excision wound model in induced diabetic and non-diabetic mice models to verify and validate the traditional wound healing claim of *C. aromatica*.

1.6.2 Objectives of the Study

The objectives of the study are:

i. To produce crude extracts of *C. aromatica* rhizomes using different solvents (n-hexane and ethanol), perform phytochemical analysis of the crude extracts, and develop and validate a new HPLC technique for quantification of curcuminoids in the rhizome extract.

ii. To perform *in vitro* screening of the crude extracts for the evaluation of potential wound healing activity: (a) antimicrobial activity, (b) antioxidant activity, (c) *in vitro* cell proliferation and viability assay using MTT, and (d) *in vitro* wound scratch assay (fibroblast bioassay).

iii. To screen polymers, formulate and characterise the extract gels of the most promising crude extract of *C. aromatica* rhizomes.

iv. To perform acute skin irritation tests for the selected formulated extract gel on mice.

v. To induce streptozotocin (STZ) diabetes in mice and perform *in vivo* studies on the induced diabetic and non-diabetic mice models to evaluate wound healing effects of the selected extract gel formulations on excision wounds.

vi. To perform histological studies to examine the extent of healing (re-epithelisation, vascularisation, and collagen deposition) of the tested formulated extract gels on the excised healed skin area of diabetic and non-diabetic mice.

CHAPTER 2

LITERATURE REVIEW

2.1 Anatomy and function of the human skin

The skin, the body's delicate outermost layer, is one of the largest human organs in terms of surface area and weight. It covers the whole human body, has a surface area of around 2 m^2 and accounts for 15-16% of the body's weight in adults, estimated at around 3.6 kg (Kolarsick *et al*., 2011; Nafisi and Maibach, 2018). Among other skin functions, it serves various critical tasks, including protection from external physical, chemical, and biological threats, preventing excessive body water loss, and assisting in temperature control (Nafisi and Maibach, 2018). It is also crucial for vitamin D production, maintaining homeostasis, and serving as a sensory organ for sensing various stimuli (Mullen, 2004; Proksch *et al*., 2008). The skin is a dynamic organ that constantly changes throughout life, as outer layer cells are shed and replaced by inner layer cells, and it comprises three structural layers (Figure 2.1): the epidermis, dermis, and hypodermis. Important skin derivatives include hair, nails, sebaceous, and sweat glands (Proksch *et al*., 2008). Skin thickness varies according to an individual's anatomical location, gender, and age. For example, the palms and soles have the thickest skin, about 4 mm thick, whereas the eyelids and postauricular regions have the thinnest, approximately 0.05 mm thick (Madison, 2003). Children's skin is thinner than adult skin, and this is because skin thickens gradually until the 40^{th} or 50^{th} decade of life, at which point it begins to thin. This thinning is predominantly a cutaneous phenomenon characterised by losing elastic fibres, epithelial appendages, and ground material (Fore, 2006).

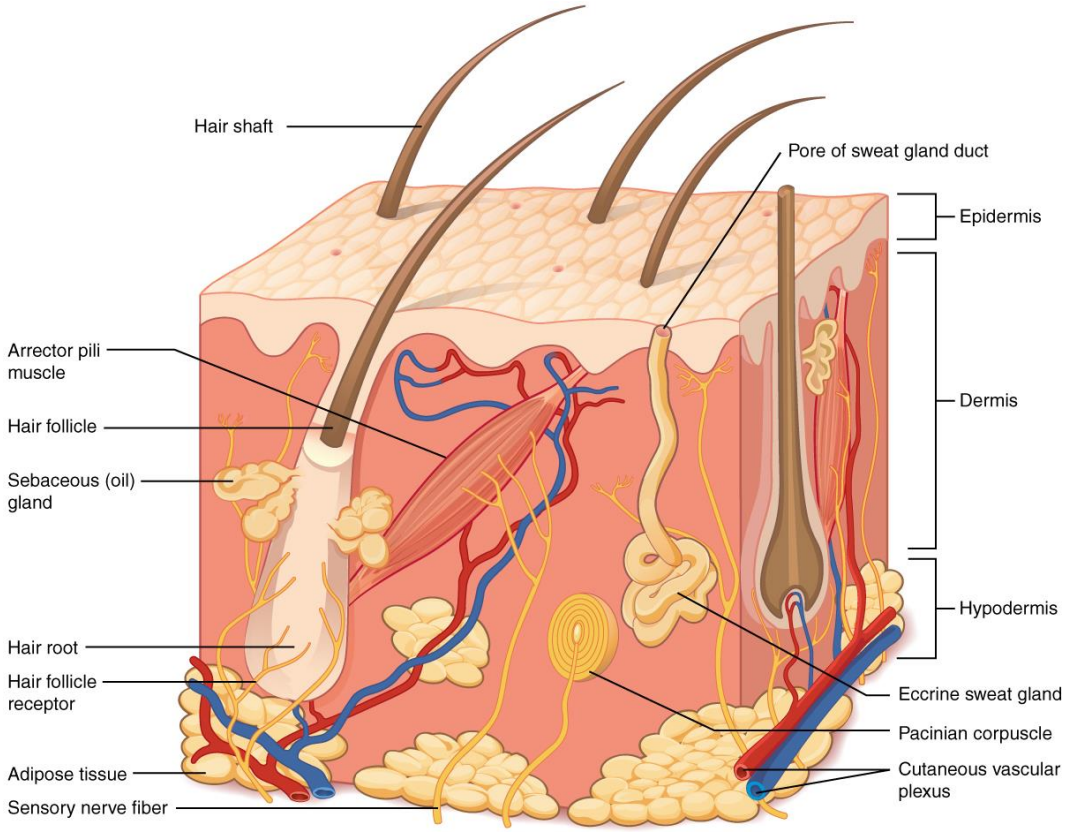

Figure 2.1: A cross-section of the skin structure showing the three layers of the skin (epidermis, dermis, and hypodermis) and its derivatives (hair, sebaceous, and sweat glands). Adapted from Umar *et al*. (2021).

2.1.1 Structure of the Skin

2.1.1.(a) The epidermis layer

The epidermis is the superficial layer of the skin and varies in thickness from the eyelid (0.5 mm) to the palms and soles (1.5 mm) (Nafisi and Maibach, 2018; Ribeiro *et al*., 2017). It is a non-vascular tissue composed of four layers of keratinocytes in different differentiation phases (Figure 2). Namely (from the deepest to the most superficial) are the basal cell layer, the spinous or squamous layer, the granular cell layer, and the stratum corneum (Honari and Maibach, 2014). The first three layers comprise the epidermis's nucleated portion, the Malpighian layer (Proksch *et al*., 2008). The stratum corneum, also called the horny cell layer, is predominantly (80%)

made up of fully keratinised cells that are no longer alive yet contribute significantly to the epidermis's homeostasis (Gilaberte *et al*., 2016). The basal layer keratinocytes are the least differentiated and the only keratinocytes in the epidermis with reproductive ability, acting as a cell reservoir and continuously providing keratinocytes to higher layers of the epidermis such as stratum spinosum, stratum granulosum, and stratum corneum through cell division and migration.

However, other non-keratinocyte cell populations of the epidermis include melanocytes, Langerhans cells, and Merkel cells (Goldsmith *et al*., 2012; Kolarsick *et al*., 2011), which will be discussed later in this chapter.

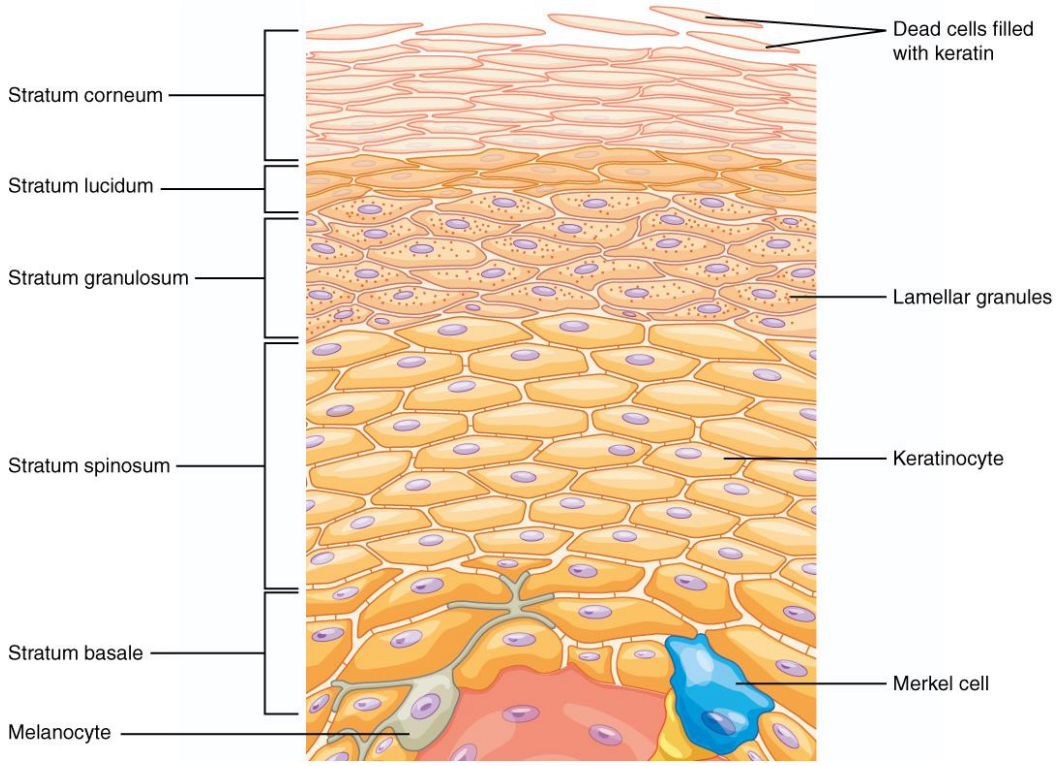

Figure 2.2: The four main layers of the epidermis's keratinocyte and other non-keratinocyte cells. Adapted with slight modification from the Wikimedia Commons (the free media repository).

The process of differentiation that happens as the cells move from lower to higher layers of the epidermis (i.e. from the basal layer to the stratum corneum) results in the formation of keratin, a component of the cytoskeleton of the cell (Chu, 2012). Multipacks of these keratin filaments congregate on and terminate at the plasma membrane to form what is known as desmosomes (intercellular attachment plates) (James *et al*., 2011). Skin secondary structures, such as nails, pilosebaceous apparatuses, and sweat glands, are derived from the epidermis (Chu, 2012; Kolarsick *et al*., 2011).

As a constantly renewing tissue, the epidermis must sustain a constant cell count while regulating epidermal cell interactions and junctions. The adhesion of keratinocytes to one another, their interactions with migrant cells, the adherence of the basal lamina to the inherent dermis, and terminal differentiation to generate corneocytes (keratinocytes without nuclei and cytoplasmic organelles) must all be controlled as cells migrate throughout life and during development (Simpson *et al*., 2011). *Morphogenesis* of the *epidermis* and differentiation are partly influenced by the underlying dermis, which is vital for the upkeep of postnatal structure and function. The epidermal-dermal junction is also a critical location for developing epidermal appendages.

The ability of epidermal cells to go through apoptosis (a programmed cell death) also plays a role in maintaining a constant epidermal thickness. Apoptosis is characterised by an ordered sequence of morphological and biochemical alterations that result in cell death without causing damage to the neighbouring cells, as frequently observed in gangrene (Escobar *et al*., 2015; Walter, 2018). Numerous cellular signalling molecules, such as growth factors, cytokines, and hormones, regulate this critical homeostatic mechanism. Apoptosis is critical in the skin for

developmental remodelling, cell number regulation, and defence against virus-infected, mutated, or differently damaged cells (Nagata, 2018; Shapouri-Moghaddam *et al*., 2018). Furthermore, terminal differentiation is an apoptotic process that transforms the keratinocyte into a defensive corneocyte (Costanzo *et al*., 2015). Disruption of the dynamic equilibrium that maintains the epidermal thickness constant can lead to psoriasis (Zhang *et al*., 2015), while dysregulation of apoptosis is frequently observed in skin tumours (Koff *et al*., 2015; Su *et al*., 2015).

2.1.1.(a)(i) Stratum germinativum

The stratum germinativum, also called the basal layer, comprises column-form keratinocytes that bind to the basement membrane area perpendicular to the dermis via their long axis. These basal cells form one layer through desmosomal junctions, bind to each other, and bind to the more superficial squamous cells (Losquadro, 2017). Additionally, basal cells are distinguished by their stretched nuclei or dark-staining oval and the existence of melanin pigment transmitted from the neighbouring melanocytes (Mauldin and Peters-Kennedy, 2015).

This basal layer of the epidermis is the hub of mitotic cells that differentiate into the outer epidermal layer's cells. Nevertheless, not every basal layer cell can divide (Zhang, 2018). In normal circumstances, stem cells of the epidermis in the basal layer are long-lived, self-renewing progenitor cells (clonogenic cells) that progress very slowly through the cell cycle (Yousef and Sharma, 2018). By stimulating stem cell division, hyperplasiogenic conditions like wounds can raise the number of epidermal cycling cells (Yang *et al*., 2019). DNA damage caused by carcinogens may result in mutations in cell proliferation machinery and may, as well, alter the speed of cell division (Kohnken *et al*., 2015). In humans, a cell in the basal

layer takes a minimum of 14 days to migrate from the basal to the cornified layer and a further 14 days from the latter (cornified layer) to reach the outermost epidermis (Sullivan and Myers, 2022).

2.1.1.(a)(ii) Stratum Spinosum (squamous cell layer)

Covering the aforementioned basal layer is a 5 to 10-cell thick epidermal layer called the stratum spinosum, also called the squamous cell layer (Yousef and Sharma, 2018). The name stratum spinosum derives from the spine-like form of the countless desmosomes on the cell borders (S. Agarwal and Krishnamurthy, 2019). This squamous layer comprises numerous cells varying in subcellular properties, shape, and structure according to location. For instance, suprabasal spinous cells have a rounded nucleus and are polyhedral in shape, while cells in the upper spinous layers are usually quite bigger, flatten out as they approach the skin's surface, and have lamellar granules (Hargis and Myers, 2017). These granules are membrane-bound organelles containing a variety of acid hydrolases, such as proteases, glycosidases, acid phosphatases, and lipases, and also contain glycoproteins, phospholipids, and glycolipids. Due to many hydrolytic enzymes, the lamellar granules appear to be a kind of lysosome. Lamellar granules act mainly in cells at the boundary between the cornified and granular layers and, in addition, act in the upper spinous layer cells, delivering precursors or source materials of the stratum corneum lipids into the intercellular space (Freeman and Sonthalia, 2019).

Keratin fibrils in the cytoplasm are organised coaxially around the nucleus and are adhered to desmosomal plaques at one edge but unbounded at the other edge closest to the nucleus (Hatzfeld *et al*., 2017; Moch *et al*., 2020). These desmosomal plaques comprise six polypeptides on the cell membrane's cytoplasm that regulate the calcium necessary for desmosomal assembly and upkeep (Hegazy *et al*., 2021;

Moch *et al*., 2020; Stahley *et al*., 2014). Desmosomes bridge the intercellular spaces between spinous cells, fostering mechanical coupling amongst epidermal cells and resisting physical stresses (Johnson *et al*., 2014). Another type of epidermal cell connection is the gap junction. These junctions enable physiologic communication through chemical signalling, which is critical for controlling cell metabolism, growth, and differentiation (Mathews and Levin, 2017; Nielsen *et al*., 2012) by forming an intercellular pore.

2.1.1.(a)(iii) Stratum Granulosum (granular cell layer)

The granular layer, also known as the stratum granulosum, amongst the epidermis's layers, is the most superficial layer containing living cells (Gilaberte *et al*., 2016). The granular layer comprises flattened cells containing plenty of keratohyalin granules in their cytoplasm. These cells are required to modify and synthesise keratinisation-related proteins further (Freeman and Sonthalia, 2019). The thickness of the granular layer varies proportionally to the thickness of the superimposed cornified layer. For instance, the granular layer beneath thin cornified layer areas might only be 1 to 3 cell layers thick, while the granular layer beneath the palms and soles may be 10-fold this thickness (Menon, 2015). However, the absence or presence of a thinly granular layer can result in extensive parakeratosis, whereby keratinocyte nuclei persist as the cells migrate into the stratum corneum, which results in a chronic skin disease called psoriasis, characterised by dry red patches covered with scales (Mauldin and Peters-Kennedy, 2015).

Keratohyalin granules are highly basophilic and have an irregular size and shape; they are needed for the formation of both the interfibrillar matrix that helps keep the keratin filaments in concert and the horny cells' inner lining (Freeman and

Sonthalia, 2019). The enzymatic action of keratohyalin granules produces soft keratin in the epidermis by cutting keratin filaments periodically. On the other hand, hair and nails lack keratohyalin granules, and as disulphide bonds are incorporated, the tonofibril filaments that traverse the cell cytoplasm harden, resulting in hard-keratin in those structures (Feng and Coulombe, 2015).

Also, because the granular layer is the epidermis keratogenous area, lysosomal enzymes are abundant in this layer and exist only in trace amounts in the stratum basalis and stratum spinosum (Nancy Ann Monteiro-Riviere, 2020). Additionally, the dissolution of cellular organelles occurs here as the granular layer cells experience a sudden terminal differentiation process into a horny cell of the cornified layer (Khiao In *et al*., 2015).

2.1.1.(a)(iv) Cornified layer

The corneocytes (horny cells) of the cornified layer offer a mechanical protective cover for the inherent epidermis and protect against invasion by foreign substances and water loss (Monteiro-Riviere, 2010). Corneocytes, which are protein-rich but low in lipids, are encased in a continuous extracellular lipid matrix (Pünnel and Lunter, 2021; Woo, 2019). These horny cells, flat, large, and polyhedral in shape, have lost their nuclei during terminal differentiation and are technically considered dead (Joffe *et al*., 2020; Mohamed and Hargest, 2022). In this layer, desmosomes are proteolytically degraded as cells protrude to the outside, contributing to the corneocyte shedding during desquamation (Évora *et al*., 2021). Cell biochemical and physical properties in the cornified layer vary depending on the position to promote desquamation outward. For example, the middle layer cells have a more remarkable ability for water binding than cells in the deeper layers, owing to

the elevated level of unbound amino acids in their cytoplasm. The deep cells are much more compressed and exhibit a wide variety of intercellular attachments than those in the more superficial layers (Mauldin and Peters-Kennedy, 2015).

2.1.1.(b) Nonkeratinocyte cells of the epidermis

2.1.1.(b)(i) Merkel cells

The Merkel cells are oviform and connected to the epidermis's basal keratinocytes via desmosomal junctions (Rickelt *et al*., 2011; Sidhu *et al*., 2005). These cells function as type-I mechanoreceptors and are found in areas of high tactile sensitivity, including lips, fingers, hair follicles-outer root-sheath, and oral cavity, and occasionally assembled into specialised structures called touch domes or tactile discs (Woo *et al*., 2015). Merkel cells are concentrated in certain parts of the body, like fingertips, resulting in some smaller, concentrated receptive fields and increased tactile sensitivity and resolution (Corniani and Saal, 2020). Merkel cells release a chemical signal in response to relatively minor deformations of adjacent keratinocytes, which causes activity in the adjacent sensory neuron, which transmits the signal to the brain (Abraham and Mathew, 2017).

2.1.1.(b)(ii) Langerhans cells

Langerhans cells are antigen-presenting dendritic cells participating in several T-cell responses (Honda *et al*., 2019). These cells originate from the bone marrow and move to a suprabasal position (which lies directly above the basal layer) in the epidermis's early stage of embryonic development, where they circulate and repopulate the epidermis throughout life (Clayton *et al*., 2017). Langerhans cells are dendritic and lack cellular junctions with adjacent cells. These cells account for 2 to 8 % of the overall epidermal cell population and retain virtually constant cell

numbers and distributions in a given area of the body (Seneschal *et al*., 2012). Langerhans cells are predominantly and primarily distributed in the squamous and granular layers of the epidermis (Clausen and Kel, 2010). Apart from the epidermis, they are also found in other squamous epithelia, such as the vagina, oral cavity, oesophagus, normal dermis and lymphoid organs (Deckers *et al*., 2018).

2.1.1.(b)(iii) Melanocytes

Melanocytes are dendritic pigment-producing cells originating from the neural crest and are found primarily in the basal layer of the skin (Ali and Naaz, 2015; Cichorek *et al*., 2013). The melanocyte's extension comes into contact with keratinocytes without forming cellular junctions as they branch into more superficial layers (Wang *et al*., 2016). Melanocytes synthesise and transport the pigment melanin to keratinocytes (Moreiras *et al*., 2021). Melanin is synthesised and stored in the melanosome, a unique intracellular organelle produced by pigment cells in the skin, through a sequence of hormone-stimulated, enzyme-catalysed, receptor-mediated reactions (Maranduca *et al*., 2019).

As reported by several authors, these melanosomes aggregate into membrane-bound melanosome complexes with two or three melanosomes in pale-skin individuals, while melanosomes are removed quickly from these complexes in keratinocytes from dark skin. Intensely pigmented skin may be the consequence of increased melanosome production, a higher level of melanisation, the existence of bigger melanosomes, better dispersion of melanosomes within keratinocytes, or a reduced rate of melanosome degradation (Benito-Martínez *et al*., 2021; D'Alba and Shawkey, 2019; Hurbain *et al*., 2018; Tadokoro and Takahashi, 2017; Thong *et al*., 2003).

2.1.2 The Dermal-Epidermal Junction

The dermis and epidermis are connected by a porous basement membrane zone that enables fluid and cell exchange and keeps the two layers together (Fenner and Clark, 2016). The dermal-epidermal junction structures are primarily composed of basal keratinocytes, and to a small extent, dermal fibroblasts are also involved (Roig-Rosello and Rousselle, 2020). The basal lamina is a layer composed primarily of collagen type-IV, anchoring filaments, and dermal microfibrils synthesised by basal cells of the epidermis. It encompasses the lamina lucida, an electron-lucent area, and the lamina densa (Joffe *et al*., 2020; Menon, 2015). Basal cells' plasma membranes are connected to the basal lamina through hemidesmosomes, which distribute tensile or shear forces throughout the epithelium. This dermal-epidermal junction serves as structural assistance for the epidermis, helps establish cell polarity and growth direction, guides the cytoskeleton arrangement in the basal cells, transmits developmental signals, and acts as a semi-permeable membrane amongst layers (Aleemardani *et al*., 2021; Briggaman and Wheeler, 1975; Burgeson and Christiano, 1997).

2.1.3 The Dermis

Just below the epidermis layer (Figure 2.1) is a thick incorporated layer of amorphous, filamentous, and fibrous connective tissue known as the dermis that allows macrophages, mast cells, fibroblasts, vascular and nerve networks, and epidermally derived appendages to gain entry in response to stimuli. Also, other blood cells, such as plasma cells, lymphocytes, and other types of leukocytes, get into the dermis in reaction to many different stimuli. The dermis represents a large percentage of the thickness of the skin and is responsible for its tensile strength,

flexibility, and elasticity. It defends the body against mechanical damage, holds water, helps in thermoregulation, and contains sensory receptors. The dermis and epidermis work together to maintain the properties of both tissues. During development, the two zones cooperate on the morphogenesis of the epidermal appendages and dermal-epidermal junction and collaborate to repair and remodel the skin as wounds heal. Although the dermis cannot differentiate in the same way as the epidermis, thus the structure and arrangement of connective tissue components are entirely predictable and depth-dependent. Collagen and elastic connective tissue components of the matrix also differ in depth and undergo turnover and remodelling in pathologic state, normal skin, and responding to an external stimulus (Brown and Krishnamurthy, 2019; Yousef and Sharma, 2018).

Almost all dermis components are of mesodermal origin, except for nerves, which originate from the neural crest, just like the melanocytes. Until around the sixth week of foetal development, the dermis is nothing more than a collection of dendritic-shaped cells containing the precursors of fibroblasts, known as acid mucopolysaccharides. Fibroblasts actively produce collagen, reticulum fibres, and elastic fibres by the 12^{th} week. By week 24, the vascular network had developed, and fat cells emerged below the dermis, eventually forming the hypodermis. The infant dermis comprises small collagen bundles, whereas the adult dermis comprises larger collagen bundles. Numerous fibroblasts exist within the dermis of infants, but only a couple survive into adulthood (Lindberg and Lamps, 2018; Sullivan and Myers, 2022).

The dermis primarily comprises collagen (type-I collagen is the most abundant), a fibrous protein family with no fewer than 15 distinct genetic types in the human skin. Collagen is the main structural protein throughout the human body and

is found explicitly in the dermis, ligaments, tendons, and bone lining. Collagen constitutes 70% of the skin's dry weight and is the skin's primary stress-resistant material (Brown and Krishnamurthy, 2019). However, elastic fibres contribute to skin flexibility and elasticity but offer little resistance to deformation and tearing (Baumann *et al*., 2021; Schmelzer and Duca, 2021), whereas proteoglycans provide hydration and viscosity (Ruiz Martínez *et al*., 2020). This extracellular matrix (ECM) of the dermis is constantly being degraded by a family member of proteases known as matrix metalloproteinases (MMPs), which are enzymes that, via a process called proteolysis, catalyse the cleaving of proteins into smaller peptide fractions and amino acids, and are replaced by new matrix constituents. These MMPs are zinc-dependent extracellular proteinases responsible for EMC remodelling (Cabral-Pacheco *et al*., 2020; Jabłońska-Trypuć *et al*., 2016). Collagenases, gelatinases, and stromelysins are the three major classes of MMPs. Collagenases are enzymes that cleave interstitial collagen, including MMP-1, MMP-8, MMP-13, and MMP-18, with MMP-1 being the most abundant. Gelatinases, including MMP-2 and MMP-9, degrade basement membrane collagens and are responsible for the denaturation of structural collagens. At the same time, stromelysins such as MMP-3, MMP-10, MMP-11, and MMP-19 are responsible for the degradation of matrix glycoproteins, proteoglycans, and basement membrane collagens as well (Almalki and Agrawal, 2016). Many authors observed that MMPs are increasingly produced in various physiological and pathologic processes, including tumour invasion, skin ageing, and wound healing (Azevedo *et al*., 2014; Caley *et al*., 2015; Freitas-Rodríguez *et al*., 2017; Rohani and Parks, 2015; Zhang *et al*., 2017a). As recently reported, keratinocytes, fibroblasts, mast cells, and neutrophils are the primary producers of these MMPs (Pittayapruek et al., 2016; Sharma et al., 2020; Stunova and Vistejnova, 2018). The balance between

MMPs and tissue inhibitors of MMPs is critical for dermal matrix structure maintenance (Cabral-Pacheco *et al*., 2020; Keane *et al*., 2018; Masciantonio *et al*., 2017). Transforming growth factor-beta (TGF-β) is a critical regulator of MMP expression, as reported in the literature (Krstic and Santibanez, 2014; Santibanez *et al*., 2018).

2.1.3(a) The Dermis Vasculature

Blood and lymph vessels perform critical homeostatic functions, including supplying nutrients to the skin and regulating the immune responses (Breslin *et al*., 2019). Blood vascularisation of the dermis is divided into a superficial horizontal plexus containing capillaries and a lower plexus (Brown and Krishnamurthy, 2019; Pichol-Thievend *et al*., 2018; Strong *et al*., 2017). Also, two plexuses are formed by the lymph vessels adjacent to the blood vascular system (Lund *et al*., 2016). The superficial lymph vessel plexus supplies the dermal papilla and drains into the larger lymph vessels to supply the lower dermis (Martinez-Corral *et al*., 2015). While the blood vessels are positioned directly beneath the epidermis, the lymph vessels are deeper inside the dermis (Breslin *et al*., 2019).

2.1.3(b) Muscles

Arrector pili (AP), the muscle fibres of arteries and veins, and the glomus bodies are the skin's involuntary (smooth) muscles (Gilaberte *et al*., 2016). The AP fibres are attached to the hair follicle underneath the sebaceous gland, pulling it vertically during contraction, and are situated in the upper dermis (Torkamani *et al*., 2017, 2014). Glomus bodies comprise an arteriovenous shunt encased in a smooth muscle cell capsule located on the fingers, toes, soles, and palms. Their prominent

role is to control the body temperature by diverting blood away from the skin's surface in cold conditions, avoiding heat loss, and enabling the maximal blood flow to the skin in hot temperatures, allowing heat to disperse (Nancy Ann Monteiro-Riviere, 2020).

Furthermore, voluntary muscles are found in the face skin, where they control facial gestures, and in the neck skin, where they are recognised as platysma, a broad sheet of muscle fibres that extend from the collarbone to the jaw angle (Hoerter and Patel, 2020; Westbrook and Varacallo, 2018).

2.1.3(c) Nerves

The autonomous nervous system is critical in preserving dermal homeostasis by controlling glandular secretions, pilomotor activities, and vasomotor functions. The skin is a vital sensory organ because it serves as the primary interface with the environment. The sensory nerve network enables the sensations of temperature, touch, itch, and pain to be perceived (Cardinali, 2018; Chokroverty and Bhat, 2021; Mota-Rojas *et al*., 2021; Smith and Johnson, 2016). In the skin, nerves are composed of both myelinated and unmyelinated fibres. Myelinated fibres are efferent neurons that connect to skeletal muscles and comprise a sub-group of afferent neurons, whereas unmyelinated fibres are autonomic and sensory fibres. Once the myelin sheaths are lost, dermal nerves end as free nerve endings, perhaps as peculiar nerve-end organs or in combination with receptors (Truini *et al*., 2015).

Meissner corpuscles are situated in the dermal papilla and are primarily found on the ventral sides of the hands and feet. Meissner corpuscles, which appear in abundance on the hands and are even more concentrated in the fingertips, help mediate touch sensing (Gill *et al*., 2017). Vater-Pacini corpuscles are large nerve-end